

## **An innovative hydrogel of gemcitabine-loaded lipid nanocapsules: when the drug is a key player of the nanomedicine structure**

Elodie Moysan, Yolanda González-Fernández, Nolwenn Lautram, Jérôme Bejaud, Guillaume Bastiat, Jean-Pierre Benoit

► **To cite this version:**

Elodie Moysan, Yolanda González-Fernández, Nolwenn Lautram, Jérôme Bejaud, Guillaume Bastiat, et al.. An innovative hydrogel of gemcitabine-loaded lipid nanocapsules: when the drug is a key player of the nanomedicine structure. *Soft Matter*, Royal Society of Chemistry, 2014, 10, pp.1767-1777. 10.1039/c3sm52781f . hal-03173115

**HAL Id: hal-03173115**

**<https://hal.univ-angers.fr/hal-03173115>**

Submitted on 18 Mar 2021

**HAL** is a multi-disciplinary open access archive for the deposit and dissemination of scientific research documents, whether they are published or not. The documents may come from teaching and research institutions in France or abroad, or from public or private research centers.

L'archive ouverte pluridisciplinaire **HAL**, est destinée au dépôt et à la diffusion de documents scientifiques de niveau recherche, publiés ou non, émanant des établissements d'enseignement et de recherche français ou étrangers, des laboratoires publics ou privés.

# An innovative hydrogel of gemcitabine-loaded lipid nanocapsules: when the drug is a key player of the nanomedicine structure

 Cite this: *Soft Matter*, 2014, 10, 1767

 Elodie Moysan,<sup>ab</sup> Yolanda González-Fernández,<sup>ab</sup> Nolwenn Lautram,<sup>ab</sup>  
 Jérôme Béjaud,<sup>ab</sup> Guillaume Bastiat<sup>\*ab</sup> and Jean-Pierre Benoit<sup>ab</sup>

A new method to form a nanoparticle-structured hydrogel is reported; it is based on the drug being loaded into the nanoparticles to form a solid structure. A lipophilic form of gemcitabine (modified lauroyl), an anti-cancer drug, was encapsulated in lipid nanocapsules (LNCs), using a phase-inversion temperature process. A gel was formed spontaneously, depending on the LNC concentration. The drug loading, measured with total entrapment efficiency, and the rheological properties of the gel were assessed. Physical studies (surface tension measurements) showed that modified gemcitabine was localised at the oil–water interface of the LNC, and that the gemcitabine moieties of the prodrug were exposed to the water phase. This particular assembly promoted inter-LNC interactions *via* hydrogen bonds between gemcitabine moieties that led to an LNC gel structure in water, without a matrix, like a tridimensional pearl necklace. Dilution of the gel produced a gemcitabine-loaded LNC suspension in water, and these nanoparticles presented cytotoxic activity to various cancer cell lines to a greater degree than the native drug. Finally, the syringeability of the formulation was successfully tested and perspectives of its use as a nanomedicine (intratumoural or subcutaneous injection) can be foreseen.

 Received 4th November 2013  
 Accepted 7th December 2013

DOI: 10.1039/c3sm52781f

[www.rsc.org/softmatter](http://www.rsc.org/softmatter)

## 1. Introduction

Gemcitabine, a nucleoside analogue of cytidine, acts against a wide range of solid tumours such as pancreatic, non-small cell lung, breast and ovarian cancers as a single agent or in combination with other agents.<sup>1</sup> Its action mechanisms are based on intracellular phosphorylation into its active phosphate derivative (by deoxycytidine kinase; dCK) after entry into the cells *via* a nucleoside transporter. An analogy with deoxycytidine triphosphate allows gemcitabine to be incorporated into DNA during replication, thus inhibiting chain elongation of DNA and causing cell death by apoptosis.<sup>2</sup> However, tumour cells often acquire resistance during gemcitabine treatment.<sup>3</sup> A lower expression of nucleoside transporters and dCK is correlated with low gemcitabine cytotoxicity.<sup>4,5</sup> Another drawback is its rapid deamination (cytidine deaminase action) to an inactive form in the blood, liver, kidney and other tissues.<sup>6</sup>

To increase its therapeutic impact, gemcitabine is administered at a high dose (1000 mg m<sup>-2</sup>) but this causes side effects.<sup>1</sup> To improve the metabolic stability and the cytotoxic activity of gemcitabine and to limit the phenomenon of resistance (lack of transporters,<sup>7</sup> alteration of dCK,<sup>8</sup> over-expression of

ribonucleotide reductase,<sup>9</sup> *etc.*), many alternatives have emerged, such as the synthesis of prodrugs<sup>10–13</sup> and the encapsulation of these prodrugs.<sup>1,14</sup> Couvreur and colleagues developed squalenoyl-gemcitabine loaded in PEGylated liposomes. These nanocarriers presented, on a subcutaneous grafted L1210wt leukaemia cell line model, similar results to *in vivo* anticancer activity with a drug dosage 5-times lower than that of free gemcitabine.<sup>15</sup> Deamination in the blood was inhibited and hence the cytotoxic efficacy was increased at lower drug concentrations.

Lipophilic forms of gemcitabine were synthesised to improve stability and cytotoxicity. Gemcitabine was covalently linked to various acyl derivatives (4-(*N*) position modification) and loaded into liposomes or lipid nanoparticles. These prodrugs were found to be more stable in plasma than the native drug and more active on KB and HT-29 cell lines (human oropharyngeal and colon carcinoma, respectively).<sup>1</sup> Lipid nanoparticles loaded with 4-(*N*)-stearoyl-gemcitabine were able to deliver the prodrug into the CCRF-CEM-AraC-8C cell line (human leukaemia), a deficient nucleoside transporter cancer cell line, whereas the native gemcitabine was unable to enter. Moreover, the loaded nanoparticles caused a cytotoxic effect 15 times higher than native gemcitabine.<sup>16</sup>

Our group has developed and patented a novel nanoscale system, so-called lipid nanocapsules (LNCs).<sup>17</sup> They are composed of lipids (triglycerides) at the core surrounded by a surfactant shell (lecithin and a pegylated surfactant) and exhibit

<sup>a</sup>LUNAM Université – Micro et Nanomédecines Biomimétiques, Université d'Angers – UMR\_S1066 (MINT), IBS-CHU Angers, 4 rue Larrey, F-49933 Angers, France. E-mail: guillaume.bastiat@univ-angers.fr; Fax: +33 (0)2 44 68 85 46; Tel: +33 (0)2 44 68 85 31  
<sup>b</sup>INSERM – U1066 IBS-CHU, F-49933 Angers, France

good dispersion stability. These biomimetic particles (analogous to lipoproteins) are obtained using an organic solvent-free phase-inversion process and their size can range from 20 to 100 nm.<sup>18</sup> Cancer treatment has been the main application for LNCs loaded with a wide variety of drugs: lipophilic anticancer drugs,<sup>19,20</sup> radionuclides<sup>21,22</sup> and genetic materials.<sup>23,24</sup> The main *in vivo* properties of these nano-objects are: the crossing of the biological barrier,<sup>25</sup> their accumulation in tumours *via* the enhanced permeability and retention (EPR) effect, and the passive targeting of lymph nodes.<sup>26</sup> Moreover, LNCs can be functionalised and combined with thiolated proteins including monoclonal Abs.<sup>27,28</sup>

The aim of this work was to successfully encapsulate gemcitabine for the first time in LNCs with an easy and organic solvent-free process. In order to optimise the cytotoxic effect of gemcitabine, the amine group was protected against deamination by adding a single 12-carbon length (C12) alkyl chain. This chemical modification permits the obtainment of a more lipophilic drug (Gem-C12) for its loading into LNCs. The lipophilic form was added during the LNC formulation process. Surprisingly, liquid LNC suspensions were not obtained in their usual form: the final product was a gel-like system. Gel properties were determined using rheological measurements *vs.* drug concentration, LNC concentration, temperature, and with additives such as urea, ethanol and NaCl. Interestingly, LNC suspensions were recovered after gel dilution. The stability of the nanocarrier and its protective effect for Gem-C12 were determined. The location of Gem-C12 inside LNCs was assessed using tensiometry, and explained the implication of the drug in the gel formation. Finally, the cytotoxicity of diluted nanocarriers and the syringeability of concentrated nanocarriers, *i.e.* gel-like structure, were tested for potential use in therapeutics as a new nanomedicine.

## 2. Materials and methods

### 2.1. Chemicals

Labrafac® WL 1349 (caprylic–capric acid triglycerides) (Labrafac) was generously provided by Gattefossé S.A. (Saint-Priest, France). Kolliphor® HS15 (formerly Solutol® HS15; mixture of free polyethylene glycol 660 and polyethylene glycol 660 hydroxystearate) (Kol) was kindly supplied by BASF (Ludwigshafen, Germany). The gemcitabine base was provided by Carbosynth (Berkshire, United Kingdom). Deionised water was obtained from a Milli-Q plus system (Millipore, Paris, France). Nile Red, Span® 80 (Span 80), Tween® 80 (Tween 80), dodecanoic anhydride, sodium chloride, urea, lauric acid, gemcitabine hydrochloride and antibiotic solutions were purchased from Sigma (St Quentin-Fallavier, France). Dulbecco's modified Eagle's medium, RMPI 1640, foetal bovine serum and horse serum were obtained from Lonza (BioWhittaker, Verviers, Belgium). (3-(4,5-Dimethylthiazol-2-yl)-5-(3-carboxymethoxyphenyl)-2-(4-sulphophenyl)-2H-tetrazolium (MTS) was purchased from Promega (Charbonnières-Les-Bains, France). Ethanol, dichloromethane and methanol were purchased from Fisher Scientific (Loughborough, United Kingdom).

### 2.2. Synthesis of 4-(*N*)-lauroyl gemcitabine

The synthesis of 4-(*N*)-lauroyl gemcitabine (Gem-C12) has already been described.<sup>11</sup> Briefly, gemcitabine base (1 mmol, 263 mg) was mixed with dioxane (16 mL) and dodecanoic anhydride (2 mmol, 765 mg) dissolved in water (4 mL) under magnetic stirring at 40 °C for 48 h. The reaction was monitored by thin-layer chromatography (dichloromethane–ethanol 96/4 v/v). Evaporation under vacuum was performed at room temperature after 24 hours to remove reaction solvents. The residue was purified by silica gel column flash chromatography (elution with a mixture of dichloromethane–ethanol 96/4 v/v). Pure fractions were gathered and evaporated under vacuum to obtain a white product, Gem-C12, as the main product. The molecular weight was analysed using a microToFQII apparatus (Bruker Daltonics GmbH, Bremen, Germany) in electrospray positive ionisation mode. <sup>1</sup>H-NMR spectra were recorded on an Avance DRX 500 MHz (Bruker Daltonics GmbH, Bremen, Germany) in deuterated dimethylsulphoxide. Elemental analysis was performed using a home-made organic microanalysis apparatus ('Service Central d'Analyse', Solaize, France).

Gem-C12 yield: 53%.

<sup>1</sup>H-NMR ((CD<sub>3</sub>)<sub>2</sub>SO): 10.99 (1H, s, NHCO), 8.22 (1H, d, 6-CH), 7.27 (1H, d, 5-CH), 6.33 (1H, m, 1'-CH), 4.16 (1H, m, 3'-CH), 3.88–3.78 (2H, m, 5'-CH), 3.65 (1H, m, 4'-CH), 2.39 (1H, t, CO-CH<sub>2</sub>), 1.52 (2H, t, CO-CH<sub>2</sub>-CH<sub>2</sub>), 1.22 (16H, m, CH<sub>2</sub>(CH<sub>2</sub>)<sub>8</sub>CH<sub>3</sub>), 0.84 (3H, t, CH<sub>3</sub>).

Elemental analysis found: C 55.32, H 7.23, N 8.99, F 8.7. Calculated for C<sub>21</sub>H<sub>33</sub>O<sub>5</sub>N<sub>3</sub>F<sub>2</sub>: C 56.63, H 7.42, N 9.44, F 8.54%.

(M + H)<sup>+</sup> *m/z* found: 446.25. Calculated: 446.23.

### 2.3. LNC preparation

The LNC formulation was based on a phase-inversion process and has already been thoroughly described.<sup>17,29</sup> The quantities of oil phase (Labrafac), aqueous phase (water and NaCl) and surfactants (Kol and Span 80) for each formulation were precisely weighed. For 30 nm-Z-Ave LNCs,  $m_{\text{Labrafac}} = 0.75$  g,  $m_{\text{Kol}} = 1.25$  g,  $m_{\text{Span80}} = 0.25$  g,  $m_{\text{Water}} = 1.02$  g and  $m_{\text{NaCl}} = 0.045$  g; for 65 nm-Z-Ave LNCs,  $m_{\text{Labrafac}} = 1.24$  g,  $m_{\text{Kol}} = 0.967$  g,  $m_{\text{Span80}} = 0.25$  g,  $m_{\text{Water}} = 1.02$  g and  $m_{\text{NaCl}} = 0.045$  g.

For the loaded-LNC formulation, Gem-C12 or lauric acid was first solubilised in a mixture of Labrafac and Span 80 at concentrations from 1 to 10% (ratio Gem-C12 or lauric acid/Labrafac w/w) at room temperature, before the addition of Kol and the aqueous phase. Mixtures were heated to 75 °C under magnetic stirring followed by cooling to 45 °C (rate of 5 °C min<sup>-1</sup>). This cycle was repeated three times and during the last temperature decrease at the phase-inversion temperature, *i.e.* 55 °C, an irreversible shock was induced by dilution with 2.12 g of pure water, urea aqueous solutions (5, 10 and 15 urea/Gem-C12 molar ratio), NaCl aqueous solutions (5, 15 and 20 NaCl/Gem-C12 n/n), or ethanol–water mixtures (5, 10 and 25 ethanol/Gem-C12 n/n). Afterwards, slow magnetic stirring was applied to the suspension of LNCs at room temperature. Gem-C12-loaded LNCs, containing Nile Red, were made by adding Nile Red (0.1% w/w Nile Red/Labrafac) before the temperature cycles.

## 2.4. Gel preparation

During slow magnetic stirring at room temperature, a hydrogel formed spontaneously, with a waxy aspect. The gelation process was considered as completed after 24 h at 4 °C. The hydrogel was diluted by a factor of 60 (v/v) with pure water. The hydrodynamic diameter (Z-Ave), polydispersity index (PDI), and zeta potential (Pz) were measured to confirm the presence of LNCs in the diluted suspensions. In addition, directly after the last dilution step of the LNC formulation, syringes with 18 Gauge ( $\varnothing$  1.2 mm) and 21 Gauge ( $\varnothing$  0.8 mm) needles were filled with the liquid suspension (before the gel formation) and stored at 4 °C for 24 h. The gels, before and after extrusion through the needles, were analysed in terms of their rheological behaviour.

## 2.5. Lipid nanocapsule characterisation

The hydrodynamic diameter: Z-average (Z-ave), polydispersity index (PDI), and zeta potential (Pz) of LNCs were determined by dynamic light scattering on a Zetasizer® Nano series DTS 1060 (Malvern Instruments S.A., Worcestershire, United Kingdom). The helium–neon laser, 4 mW, was operated at 633 nm, with the scattering angle fixed at 173° and the temperature at 25 °C. The curve fittings of the correlation functions were performed using an exponential fit (Cumulant approach) for Z-Ave and PDI determinations for the LNC suspensions. Smoluchowski's approximation was used to determine the electrophoretic mobility for Pz determination.

## 2.6. Evaluation of drug loading efficacy

The drug loading and entrapment efficiency were determined using the UPLC method. Gem-C12 concentrations loaded into LNCs were determined after dialysis: 2 mL of LNC preparation was filtered (0.2  $\mu$ m) and was poured into a dialysis tube (cut-off of 100 kDa) and inserted into a 4000 mL flask containing deionised water at 25 °C and maintained under magnetic stirring (300 rpm). The amount of drug in the dialysis tube was determined after the disruption of LNCs by using methanol (1 : 36 v/v). As a control, total quantities of Gem-C12 added to the formulation were determined without filtration and dialysis, by the disruption of LNCs using methanol.

A UPLC apparatus was equipped with a UV spectroscopy detector. The samples were injected into a C18 column (1.7  $\times$  100 mm, ACQUITY UPLC BEH C18) equipped with a column guard. The column was eluted (methanol as the elution solvent) at 0.343 mL min<sup>-1</sup> flow rate. The detection wavelength was 248 and 266 nm. Peak heights were recorded and processed on MPower software (Waters, USA). The drug concentration was calculated from a linear titration curve, with freshly made Gem-C12 methanol solutions at a concentration range from 1 to 100  $\mu$ g mL<sup>-1</sup>.

## 2.7. Rheological properties

The viscoelastic properties of the gels at room temperature were measured using a Kinexus® rheometer (Malvern Instruments S.A., United Kingdom), with a cone plate geometry (diameter 40 mm, angle: 2°). A parallel plate geometry (diameter 20 mm, gap:

700  $\mu$ m) was used for temperature experiments. Oscillatory strain sweeps at 1 Hz constant frequency were performed to determine the linear regime characterised by constant dynamic moduli (storage modulus:  $G'$  and loss modulus:  $G''$ ), independent of the strain amplitude. In this regime (0.1% constant strain),  $G'$  and  $G''$  were measured as a function of angular frequency (0.1 to 100 Hz). The solid-to-liquid temperature ( $T_{SL}$ ) transition was determined at a constant frequency and strain, 1 Hz and 0.01%, respectively, in a range of temperatures from 4 to 60 °C and at a heating rate of 2 °C min<sup>-1</sup>. All these experiments were repeated three times.  $G'$ ,  $G''$  and  $T_{SL}$  values were expressed as the mean  $\pm$  standard deviation (SD).

## 2.8. Tensiometry

Absorption kinetics were obtained at the Labrafac–water interface by means of a rinsing drop method using a drop tensiometer device (Tracker Teclis, Longessaigne, France). For this study, Gem-C12 was diluted in Labrafac, from 0 to 6 mg g<sup>-1</sup> (Gem-C12/Labrafac w/w). Basically, a Labrafac drop (5  $\mu$ L) was formed with an Exmire microsyringe (Prolabo, Paris, France) in an optical glass bowl (Hellma, Paris, France) containing a water phase. The axial symmetric shape (Laplacian profile) of the drop was analysed by using a video camera connected to a microcomputer. From numerical image analysis, with the Laplace equation integrating the drop profile points, the interfacial tension, the surface area and the volume of the drop were recorded in real time (five measurements per second). Piston movements of the syringe were controlled by a stepping motor connected to a microcomputer, to control the drop volume and to keep the surface area constant. Absorption kinetics consisted of the formation of a monolayer by the gradual diffusion of the amphiphilic molecules from the drop's core to the interface, until complete saturation was achieved. Saturation was reached when the surface tension stabilised. For each Gem-C12 concentration, experiments were repeated in triplicate and the surface tension was expressed as the mean  $\pm$  SD.

## 2.9. LNC release from the gel dissolution

Gem-C12-loaded LNCs in the gel form, containing Nile Red, were used to study the release of LNCs from the gel. Directly after the LNC formulation, 200  $\mu$ L of LNC suspension was placed in a spectrometry container to form a hydrogel (one night at 4 °C). PBS (1.8 mL at pH 6.5 or 7.4), preheated at 37 °C, was added on top of the hydrogel and the containers were incubated at 37 °C. 200  $\mu$ L samples of buffer were collected and replaced by 200  $\mu$ L of pre-heated PBS to maintain a constant volume. Hydrogel dissolution (presence of LNCs in buffer) was followed by fluorescence (Fluoroskan, Ascent, Thermo Fisher Scientific, Courtaboeuf, France) (ex/em 515/590 nm) and the size distribution was measured. The total hydrogel dissolution (100% of LNCs in suspension) was obtained by fluorescence, mixing 200  $\mu$ L of Gem-C12-loaded LNCs containing Nile Red in suspension (directly after the LNC formulation) with 1.8 mL of PBS. All the experiments were repeated 3 times.

## 2.10. Cell culture

Human pancreatic carcinoma Mia PaCa-2 and BxPc-3, and human lung cancer H460 cell lines were obtained from ATCC (Manassas, VA, USA). Mia PaCa-2 cells were cultured in Dulbecco's modified Eagle's fortified medium containing glucose ( $4.5 \text{ g L}^{-1}$ ) whereas BxPc-3 and H460 cells were cultured in RPMI 1610. All media were completed with foetal bovine serum (10% v/v), horse serum (2.5% v/v, only for Mia PaCa-2 culture), penicillin ( $100 \text{ UI mL}^{-1}$ ), streptomycin ( $100 \mu\text{g mL}^{-1}$ ) and amphotericin B ( $0.250 \mu\text{g mL}^{-1}$ ). The fresh medium was substituted every 48 h. When cells reached 80% confluence, dissociation was performed using trypsin and replated in  $75 \text{ cm}^2$  flasks, at  $37^\circ\text{C}$  in a  $\text{CO}_2$ -air mixture (5/95 v/v).

## 2.11. Proliferation assay

The cytotoxicity of diluted Gem-C12-loaded LNCs was determined using the MTS test. Fresh medium, empty LNCs, gemcitabine hydrochloride and pure Gem-C12 (in water-ethanol-Tween 80 87.6/5.5/6.9 (v/v)) were used as controls. Cells were seeded into 96-well plates (15 000 cells per well) and incubated at  $37^\circ\text{C}$  in a  $\text{CO}_2$ -air mixture (5/95 v/v) overnight. Various amounts of drugs (maximum concentration values of 250, 100 and  $50 \mu\text{M}$  for Mia PaCa-2, BxPc-3 and H460, respectively) and LNCs were added into the wells, and the cells were incubated for 48 h.

The number of living cells was determined using an MTS assay (colorimetric assay based on the conversion of a tetrazolium salt into formazan). Formazan absorbance was measured at 492 nm and 750 nm, directly from 96-well plates using a spectrophotometer (Multiscan Ascent MP reader, Thermo Scientific, Courtaboeuf, France), after exposition to MTS ( $20 \mu\text{L}$  per well) for 2.5 h at  $37^\circ\text{C}$ . The percentage of cell viability was calculated according to the following equation:

$$\text{Cell viability (\%)} = \frac{\text{Abs(T)}}{\text{Abs(C)}} \times 100$$

with Abs (T) and Abs (C), the absorbency values of treated and untreated cells (with fresh medium), respectively. The quantity of formazan is proportional to the number of living cells in the culture. The relative percentage of living cells (compared to living cells with fresh medium control) was reported as the mean  $\pm$  SD of three different experiments.

## 2.12. Statistical analysis

All results were expressed as the mean  $\pm$  SD. Normal distributions were assumed for the rheological moduli  $G'$  and  $G''$ . Significant differences between means of rheological moduli were analysed by one-way analysis of variance (ANOVA 1F), followed by Scheffe's *post hoc* test for pairwise comparisons. Differences were considered statistically significant for  $p < 0.05$ .

# 3. Results and discussion

## 3.1. Gem-C12-loaded LNC gel technology

The phase-inversion temperature (PIT) method was first described by Shinoda<sup>30</sup> and developed by Heurtault<sup>29</sup> to obtain

nano-objects based on an oily core (Labrafac) surrounded by an organised assembly made of lecithin molecules and PEGylated surfactants (Kol) with the PEG chains oriented towards the aqueous phase.<sup>17,29</sup> A similar process was used, changing lecithin with Span 80. After the temperature cycles and the rapid cooling dilution, LNC suspensions were obtained (Fig. 1 inset A). By changing Labrafac and surfactant compositions, LNC hydrodynamic diameters (Z-Ave) were modified:  $30.0 \pm 0.5$  and  $67.0 \pm 2.0$  nm. The PDI was lower than 0.1 for all these nano-objects ( $0.05 \pm 0.01$  and  $0.04 \pm 0.01$ , respectively), characteristic of a monomodal and thin size distribution. Pz values were  $-9.3 \pm 4.6$  mV and  $-7.5 \pm 3.0$  mV, respectively, and corresponded to classical values obtained for LNCs.<sup>17</sup>

Gemcitabine hydrochloride, a hydrophilic drug, is not easy to encapsulate inside LNCs. Due to the lipophilic core, encapsulation strategies have to be developed for this purpose as already performed by our group (reverse micelle, aqueous core LNCs) for other molecules.<sup>31,32</sup> The hydrophobisation of gemcitabine could also be an appropriate approach as described in the literature.<sup>14,33</sup> Lauroyl-modified gemcitabine (Gem-C12) was synthesised and the characterisation data are given in the 'Materials and methods' section. To obtain Gem-C12-loaded LNCs, the drug was first added to the initial mixture before the first temperature cycle. The drug concentration was modified from 1 to 10% (Gem-C12/Labrafac w/w). After the rapid cooling dilution, suspensions were obtained but they turned into a waxy gel (Fig. 1 inset B) for drug concentrations higher than 5%. Below this drug concentration value, no gelation occurred and a LNC suspension was always obtained.

Gels could be dissolved in an excess of water and nano-objects were still visible, showing the physical character of the gel association. For the corresponding 67 nm-Z-Ave blank LNC composition, the loaded nano-object Z-Ave was  $55.5 \pm 2.0$  nm,

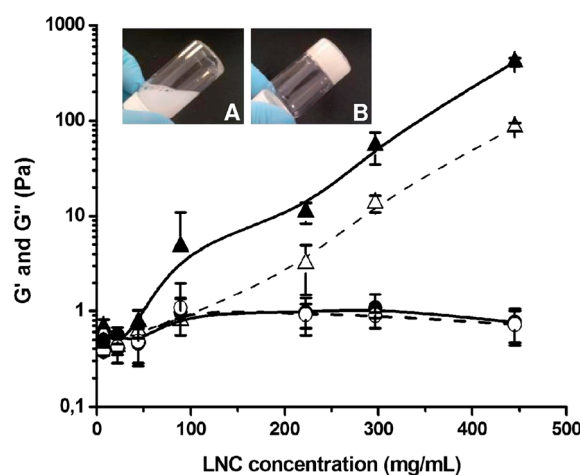


Fig. 1 Storage modulus  $G'$  (closed symbols, solid lines) and loss modulus  $G''$  (open symbols, dotted lines) vs. LNC concentration for Gem-C12 5% (Gem-C12/Labrafac w/w) loaded ( $\blacktriangle$ ,  $\triangle$ ) and non-loaded LNCs (Z-Ave = 67 nm) ( $\bullet$ ,  $\circ$ ) ( $n = 3$ , mean  $\pm$  SD). Non-loaded LNC suspension (inset A) and Gem-C12-loaded LNC gel (inset B) pictures at room temperature (LNC concentration  $445 \text{ mg mL}^{-1}$ ; 5% Gem-C12/Labrafac w/w).

with a PdI and Pz of  $0.05 \pm 0.01$  and  $-8.0 \pm 2.5$  mV, respectively. For the corresponding 30 nm-Z-Ave blank LNC composition, the loaded nano-object Z-Ave was similar:  $29.0 \pm 1.0$  nm, with a PdI and Pz of  $0.03 \pm 0.02$  and  $-3.0 \pm 0.3$  mV, respectively.

Gem-C12 encapsulation rates were determined using the UPLC method after LNC disruption in methanol, with and without filtration and dialysis. Whatever the Gem-C12 concentration, the drug was totally encapsulated into the nano-objects. No difference in Gem-C12 loading was observed: (i) directly after the formulation process (initial Gem-C12 loading) and (ii) after the filtration (large Gem-C12 aggregate elimination) followed by the dialysis process (residual micelle elimination). The total encapsulation rate, size, PdI and Pz of nano-objects were constant over time (1 year) at 4 °C, whatever the storage form of this innovative pharmaceutical technology: gel state or diluted state.

### 3.2. Rheological characterisation

Rheological analysis (viscoelastic property characterisation) was performed for Gem-C12-loaded LNCs in the gel state, changing the applied strain at a constant oscillation frequency of 1 Hz. Whatever the drug loading, all gels presented a linear regime corresponding to strain-independent storage ( $G'$ ) and loss ( $G''$ ) moduli up to a critical strain value of about 1%. Beyond this critical value,  $G'$  and  $G''$  decreased.

The viscoelastic properties of the gels were then studied at 25 °C, within the linear regime (0.1% strain), as a function of the oscillation frequency. Constant values were obtained from 0.02 to 8.0 Hz, characteristic of a gel state.  $G'$  and  $G''$  profiles vs. Gem-C12-loaded LNC (5% Gem-C12/Labrafac w/w) concentrations are illustrated in Fig. 1. Without any additional volume for shock dilution at the end of the formulation process, *i.e.* Gem-C12-loaded LNC concentration of  $445 \text{ mg mL}^{-1}$ , the  $G'$  and  $G''$  values were  $410 \pm 40$  and  $90 \pm 10$  Pa, respectively. The  $G'/G''$  ratio was about 4.5, showing the strong elasticity of the gel.

Similar results were obtained by dilution of the gel or by using various volumes of shock dilution at the end of the formulation process. When the gel was diluted,  $G'$  and  $G''$  significantly decreased ( $p < 0.01$ ) up to  $5 \pm 6$  and  $1 \pm 1$  Pa, respectively, for a Gem-C12-loaded LNC concentration of  $89 \text{ mg mL}^{-1}$ . Gel hardness was lost with dilution but elasticity remained constant:  $G'/G''$  was about 5 for a Gem-C12-loaded LNC concentration of  $89 \text{ mg mL}^{-1}$ . No gelation and no elastic behaviour were observed with the corresponding non-loaded LNCs, considering the same LNC concentration range. At concentrations lower than  $89 \text{ mg mL}^{-1}$ , Gem-C12-loaded and non-loaded LNCs have the same rheological behaviour with  $G'$  and  $G''$  values close to 1 Pa corresponding to the absence of gelation and consequently the absence of elastic behaviour.

$G'$  and  $G''$  profiles, *i.e.* the gel hardness, were dependent on the Gem-C12 concentration (Gem-C12/Labrafac w/w) (Fig. 2A).  $G'$  and  $G''$  values increased by about 1 decade when the drug

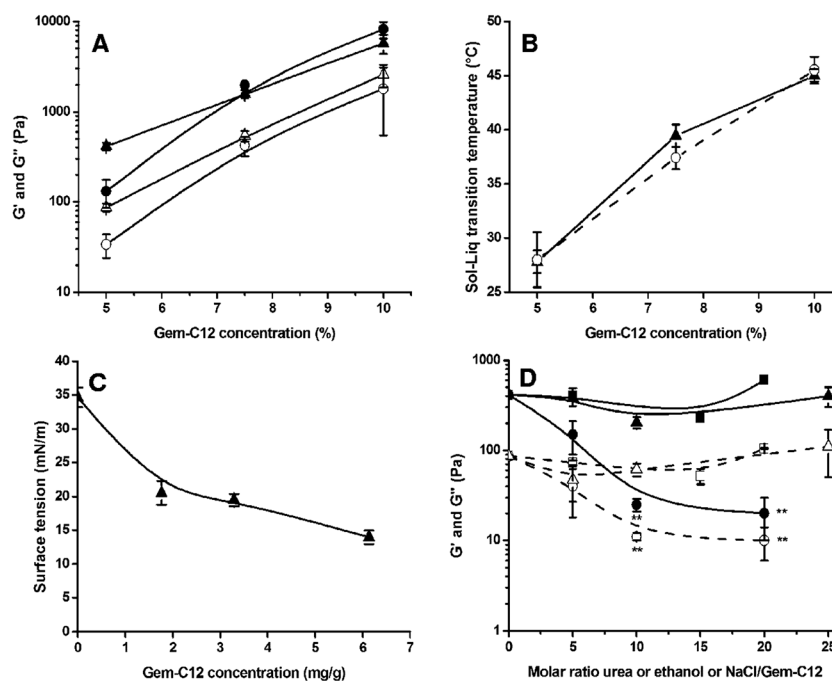


Fig. 2 (A) Storage modulus  $G'$  (closed symbols, solid lines) and loss modulus  $G''$  (open symbols, dotted lines) vs. Gem-C12 concentration (Gem-C12/Labrafac w/w) for 29 nm-Z-Ave (●, ○) and 55 nm-Z-Ave (▲, △) Gem-C12-loaded LNCs. (B) Solid-to-liquid transition temperature  $T_{SL}$  vs. Gem-C12 concentration (Gem-C12/Labrafac w/w) for 29 nm-Z-Ave (○) and 55 nm-Z-Ave (▲) Gem-C12-loaded LNCs. (C) Surface tension of the Labrafac–water interface of a 5  $\mu\text{L}$  Labrafac drop in water vs. Gem-C12 concentration (Gem-C12/Labrafac w/w). (D) Storage modulus  $G'$  (closed symbols, solid lines) and loss modulus  $G''$  (open symbols, dotted lines) for Gem-C12-loaded LNCs (Z-Ave = 55 nm, Gem-C12 concentration = 5% Gem-C12/Labrafac w/w) vs. the molar ratio of urea (●, ○) or ethanol (▲, △) or NaCl (■, □) with Gem-C12 ( $n = 3$ , mean  $\pm$  SD; \*\*:  $p < 0.01$ ).

concentration increased from 5 to 10%, whatever the studied Gem-C12-loaded LNC size. Drug concentrations of 5%, 7.5% and 10% had no effect on gel elasticity, with a relatively constant  $G'/G''$  ratio of about 4.5, 2.9 and 2.2, respectively, for the LNC Z-Ave of 55 nm and 3.9, 4.7 and 4.5, respectively, for the LNC Z-Ave of 29 nm. Moreover, gel properties were independent of the Gem-C12-loaded LNC size. Similar  $G'$  and  $G''$  modulus values were observed for the Gem-C12-loaded LNC Z-Ave of 29 nm and 55 nm, at a constant Gem-C12 concentration of 5 to 10% (Gem-C12/Labrafac w/w).

Gel properties ( $G'$  and  $G''$ ) were studied *vs.* temperature at a constant oscillation frequency (1 Hz) and constant strain (0.01%). A solid-to-liquid temperature ( $T_{SL}$ ) transition ( $G'$  and  $G''$  crossing) was observed, depending on the Gem-C12 concentration (data not shown). From 5 to 10% drug concentration (Gem-C12/Labrafac w/w),  $T_{SL}$  linearly increased from about 30 to 45 °C (Fig. 2B). While drug concentration effects were observed, no dependence on the Gem-C12-loaded LNC Z-Ave was shown (Fig. 2B).  $T_{SL}$  were about  $45 \pm 1$  and  $46 \pm 1$  °C for 29 and 55 nm Z-Ave of loaded LNCs, respectively (10% Gem-C12/Labrafac w/w).

To sum up, Gem-C12 concentrations in LNCs and Gem-C12-loaded LNC concentration influenced the  $G'$  and  $G''$  gel properties and  $T_{SL}$ , *i.e.* the gel state to LNC suspension transition, while no influence was shown with Gem-C12-loaded LNC size.

### 3.3. Surface tension measurements

A Labrafac–water interface study was performed using a 5  $\mu$ L Labrafac drop in water. The surface tension was measured at the Labrafac–water interface *vs.* the Gem-C12 concentration (Gem-C12/Labrafac w/w), when the drug was solubilised in the Labrafac drop (Fig. 2C). As the drug concentration was increased from 0 to 6 mg g<sup>-1</sup>, the surface tension significantly decreased from  $34.6 \pm 1.5$  to  $14.0 \pm 1.0$  mN m<sup>-1</sup>, respectively. Gem-C12 behaves as an amphiphilic molecule and moves from the oil drop to the Labrafac–water interface.

### 3.4. Interaction characterisation in the gel state

Lauric acid was encapsulated in a similar manner as for Gem-C12. An LNC suspension was obtained at the end of the process, without any gelation.  $G'$  and  $G''$  values for the 5% lauric acid-loaded LNC (lauric acid/Labrafac w/w, Z-Ave =  $62.5 \pm 0.4$  nm) suspension were about 1 Pa, similar to values obtained with blank LNCs (Fig. 1). So the gemcitabine moiety, from the Gem-C12 molecule, was responsible for the nano-object gelation.

Ethanol, NaCl, or urea was added during the formulation process (in the shock dilution process) of 5% Gem-C12-loaded LNCs (Gem-C12/Labrafac w/w, Z-Ave =  $55.0 \pm 0.2$  nm) to characterise the LNC interactions implied during gelation. While no significant difference was observed when ethanol or NaCl was added, the addition of urea significantly decreased the gel hardness (Fig. 2D). Modulus values decreased from  $410 \pm 40$  ( $G'$ ) and  $90 \pm 10$  ( $G''$ ) without urea to  $21 \pm 10$  ( $G'$ ) and  $10 \pm 4$  Pa ( $G''$ ) with a urea/Gem-C12 molar ratio of 20. Therefore, gelation between Gem-C12-loaded LNCs was due to H-bonds.

Electrostatic or van der Waals interaction can be rejected (no effect of NaCl and ethanol, respectively).<sup>34,35</sup>

### 3.5. Gel property and *in vitro* syringe injection

As part of pharmaceutical development, this innovative gel form could be injected subcutaneously or locally into patients. To avoid surgery, this form should be injected using a syringe, and the gel property has to be recovered after extrusion through thin needles. Feasibility was performed, filling syringes directly after the shock dilution at the end of the formulation (before gelation occurred). Then, once the gel was formed inside the syringe, the material was directly extruded through 18 and 21 G needles in a rheometer.

Fig. 3 reports  $G'$  and  $G''$  values for the Gem-C12-loaded LNC gel (445 g mL<sup>-1</sup> constant LNC concentration) with various drug concentrations: 5, 7.5 and 10% (Gem-C12/Labrafac w/w) and for

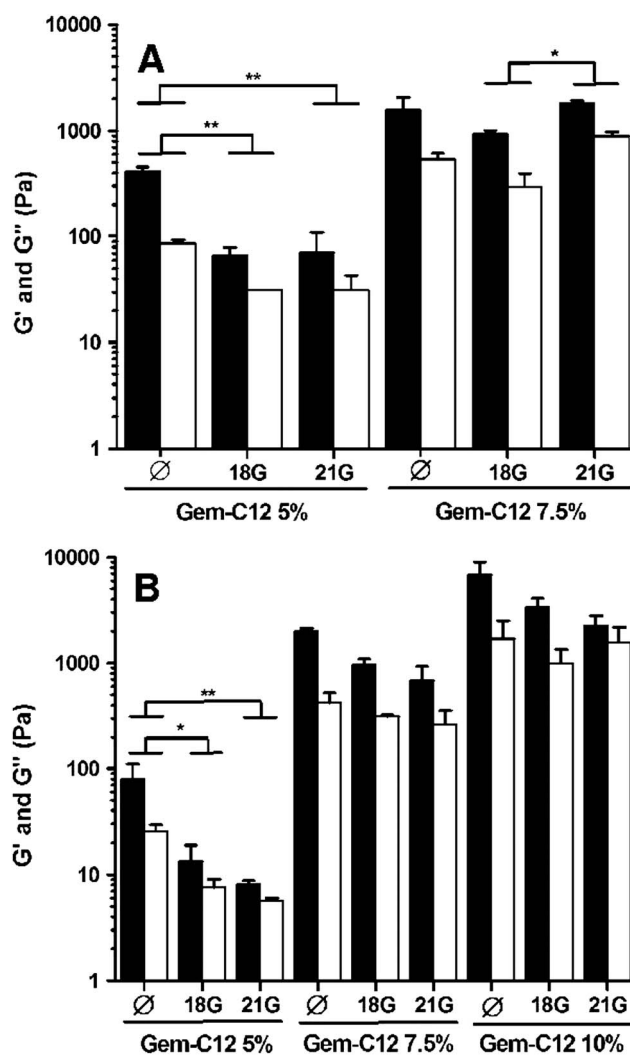


Fig. 3 Storage modulus  $G'$  (black bars) and loss modulus  $G''$  (white bars) for Gem-C12-loaded LNCs (Z-Ave = 55 (panel A) and 29 nm (panel B), Gem-C12 concentration = 5, 7.5 and 10% Gem-C12/Labrafac w/w, LNC concentration 445 mg mL<sup>-1</sup>) before ( $\emptyset$ ) and after extrusion through 18 G and 21 G-needles ( $n = 3$ , mean  $\pm$  SD; \*:  $p < 0.05$ , \*\*:  $p < 0.01$ ).

the 29 and 55 nm LNC Z-Ave. Comparisons were assessed without and after extrusion. Whatever the LNC Z-Ave and needle size, no significant difference was observed before and after extrusion when the drug concentrations were 7.5 and 10% (Gem-C12/Labrafac w/w). For a 5% drug concentration, a significant  $G'$  and  $G''$  decrease was observed without and after extrusion through needles. Nevertheless, the liquid form was not recovered. For the 29 and 55 nm Z-Ave loaded LNC gel,  $G'$  and  $G''$  values were 1 and 2 decades higher than for non-loaded LNCs, respectively. Feasibility with a 55 nm Z-Ave loaded LNC gel with 10% drug concentration (Gem-C12/Labrafac w/w) was not performed due to the instantaneous gelation process directly after the shock dilution at the end of the formulation, and hence the impossibility to fill the syringes.

### 3.6. *In vitro* hydrogel dissolution

*In vitro* hydrogel dissolution studies were performed in order to follow the release of LNCs from the hydrogel. When the hydrogel of LNCs loaded with 5% of Gem-C12 (Gem-C12/Labrafac w/w) was in contact with PBS, rapid dissolution occurred and reached 100% of LNCs in suspension at 6 h and 24 h with the LNC Z-Ave of 29 and 55 nm, respectively (Fig. 4A and B). No difference was observed when changing the pH from 7.4 to 6.5. For LNCs loaded with 7.5% of Gem-C12 (Gem-C12/Labrafac w/w), a slower dissolution was observed. About 50% of LNCs were in suspension after 48 h for the two LNC Z-Aves. After 1 week, about 70% of LNCs were in suspension with a LNC Z-Ave of 29 nm whatever the pH, while about 60 and 50% of LNCs in suspension at pH 6.5 and pH 7.4, respectively, were observed for a LNC Z-Ave of 55 nm. There was no change in LNC Z-Ave in suspension over time, whatever the pH (6.5 and 7.4) when the hydrogel was dissolved (data not shown).

### 3.7. *In vitro* cytotoxicity of Gem-C12-loaded LNCs on tumour cells

*In vitro* cytotoxicity was tested vs. Gem-C12 concentration on three tumour cell lines: a human lung cancer: H460, and two pancreatic cancers: BxPc-3 and Mia PaCa-2. Mia PaCa-2 is known to be resistant to gemcitabine whereas BxPc-3 and H460 seem to be more sensitive to this drug.<sup>36,37</sup> Four formulations were tested: gemcitabine hydrochloride in aqueous solution, Gem-C12 in a mixture of water-ethanol-Tween 80 (87.6/5.5/6.9 v/v/v), non-loaded LNCs (Z-Ave = 67 nm) and Gem-C12-loaded LNCs (Z-Ave = 55 nm, Gem-C12 concentration = 5% Gem-C12/Labrafac w/w) in a liquid form after gel dilution (Fig. 5A–C).

After 48 h of exposure to Gem-C12-loaded LNCs at 37 °C, the cell viability decreased. Gem-C12-loaded LNCs were incubated with Mia PaCa-2, BxPc-3 and H460 and the half maximal inhibitory concentrations ( $IC_{50}$ ) were measured at 125, 1 and 0.5  $\mu$ M respectively. No cytotoxicity was observed for non-loaded LNCs in the concentration range studied. To extrapolate from the Gem-C12 concentration, this non-loaded nanocarrier suspension was similarly diluted to Gem-C12-loaded LNC levels. *In vitro* cytotoxicity observed with Gem-C12-loaded LNCs was due to the drug and not the nanocarrier alone. After incubation, close  $IC_{50}$  values for Gem-C12 without LNC nanocarriers

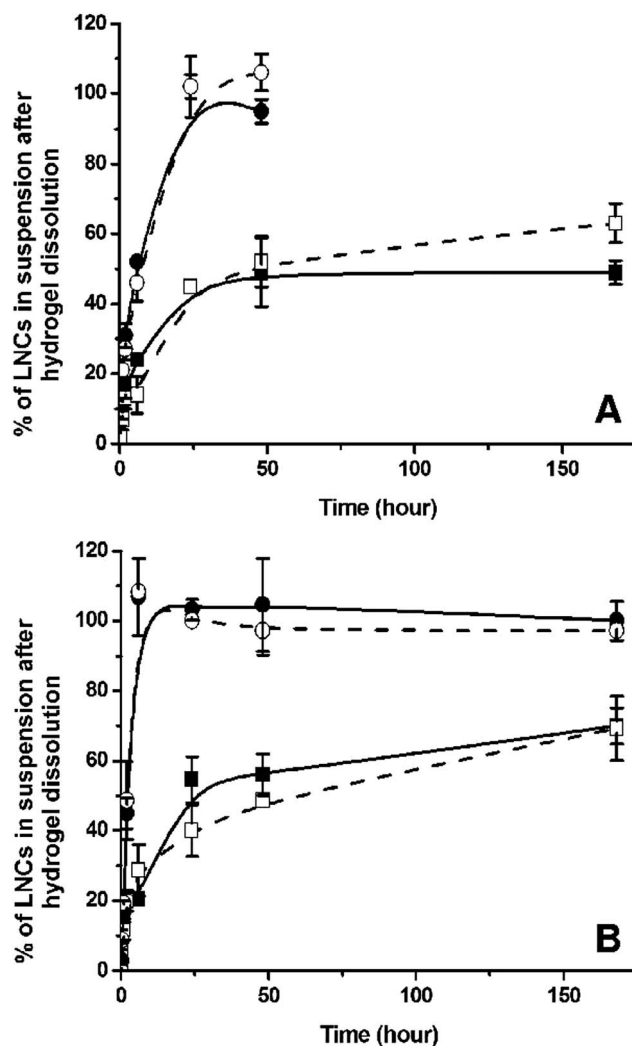


Fig. 4 % of LNCs generated from hydrogel dissolution after incubation in PBS at 37 °C, at pH = 7.4 (closed symbols, solid lines) and pH = 6.5 (open symbols, dotted lines). LNC Z-Ave of 55 (panel A) and 29 nm (panel B) were loaded with various concentrations of Gem-C12 (●, ○: 5% and ■, □: 7.5% Gem-C12/Labrafac w/w) ( $n = 3$ , mean  $\pm$  SD).

and for Gem-C12-loaded LNCs were observed. Gemcitabine hydrochloride presented a high level of cytotoxic behaviour on the BxPc-3 cell line, with an  $IC_{50}$  value of about 1  $\mu$ M (Fig. 5B). On the other hand, no cytotoxic effect was found when gemcitabine hydrochloride was incubated with Mia PaCa-2, up to 250  $\mu$ M of drug concentration was used. With these three cancer cell lines, a significant increase of sensitivity was observed with Gem-C12 alone or Gem-C12-loaded LNCs compared to the commercialised drug (gemcitabine hydrochloride).

### 3.8. Discussion

In the 1990's, innovative gel materials were reported in the field of pharmaceutical technology. These materials, called organogels, are ternary mixtures of oil, water and low-molecular-weight molecules (lecithin, sorbitan monostearate, or monopalmitate) and the ternary composition was adjusted to obtain solid-like



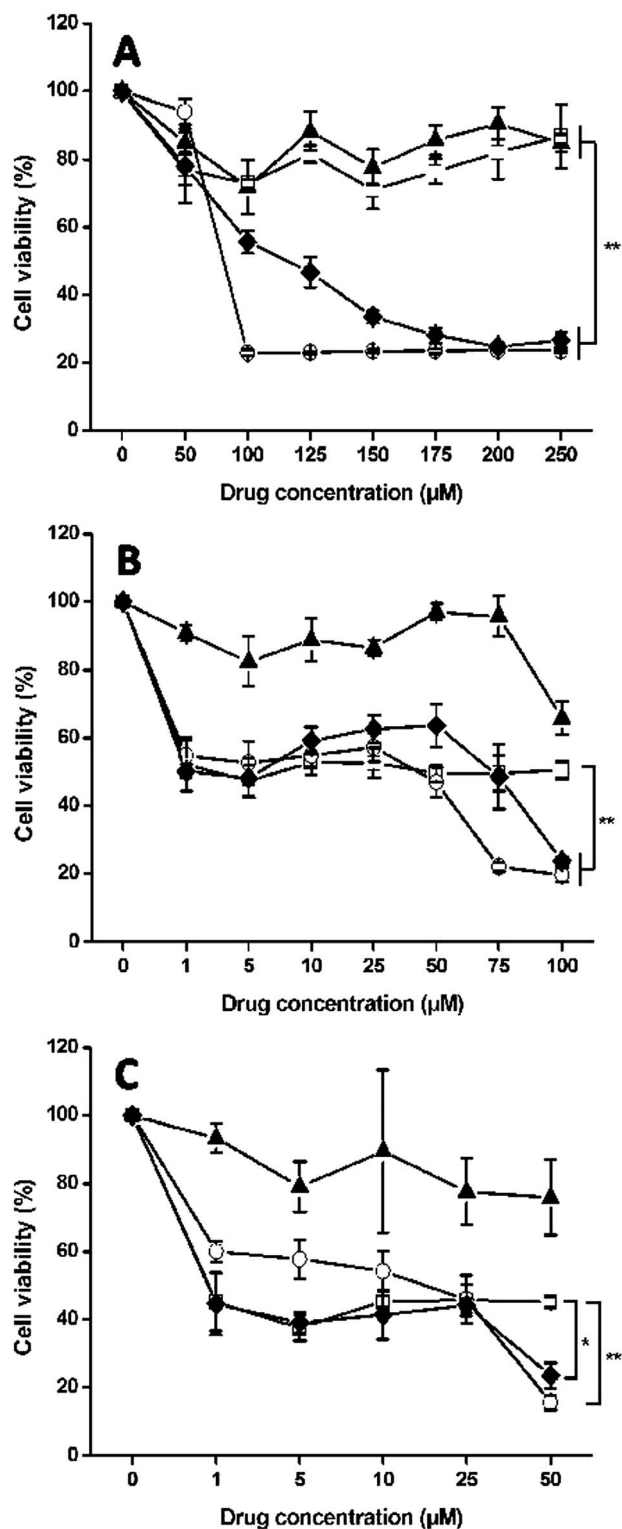


Fig. 5 Cell viability of Mia PaCa-2 (panel A), BxPc-3 (panel B) and H460 (panel C) cell lines vs. drug concentration after 48 h incubation (37 °C) with Gem-C12 (○) (solution in water–ethanol–Tween 80 87.6/5.5/6.9 v/v/v), gemcitabine hydrochloride (□) (solution in PBS), Gem-C12-loaded LNCs (◆) (Z-Ave = 55 nm, Gem-C12 concentration = 5% Gem-C12/Labrafac w/w) and non-loaded LNCs (▲) (Z-Ave = 67 nm). There is no Gem-C12 inside non-loaded LNCs, but dilutions were performed in the same way as that for Gem-C12-loaded LNCs for comparison ( $n = 3$ , mean  $\pm$  SD; \* $p < 0.05$ , \*\* $p < 0.01$ ).

systems.<sup>38–43</sup> *In vitro* release and *in vivo* efficacy were assessed for propranolol,<sup>44</sup> cyclosporin A<sup>45</sup> and antigen models (bovine serum albumin and haemagglutinin)<sup>40,41,46</sup> for nasal, oral, subcutaneous and intramuscular administration. Clinical trials for transdermal diclofenac administration were also reported.<sup>47–49</sup> No dilution matrix description was reported for the organogel described previously. The nature of the gel architecture, *i.e.* a gelling network composed of entangled rod-shaped tubules (entangled cylindrical reverse micelles), was described.<sup>39,43,50</sup> The organogel dilution should lead to an oil/water phase separation. Similar systems were obtained with the ternary mixture of Labrafac (oil), water, Kolliphor/Span 80 (low-molecular-weight molecules) when Gem-C12 was added to the formulation. Nevertheless, the innovation of this system is the re-obtention of nanoparticles after dilution of the gels. The gel architecture developed in this study is new. It consists of the inter-nanoparticle association of Gem-C12-loaded LNCs with H-bond cross-linkings between the gemcitabine moieties of Gem-C12 located at the oil–water interface of LNCs (Fig. 2C and D). The gemcitabine moiety of Gem-C12, oriented towards the water phase, was therefore responsible for the gel formation; a schematic representation of the gel structure could be a tridimensional pearl necklace immobilising the water phase. Once diluted, the necklace breaks and the pearls (Gem-C12-loaded LNCs) are recovered in the water phase, with the subsequent loss of gel rheological properties (Fig. 1). In the present study, the gelation among Gem-C12-loaded LNCs is due to physical interactions and a reversible solid-to-liquid temperature ( $T_{SL}$ ) transition was observed (Fig. 2B), confirming the presence of H-bonds.<sup>51</sup>

The gel material developed in this study could be considered as a hydrogel. Indeed, hydrogels may be defined as semi-solid formulations having an external polar phase, immobilised within the spaces available of a three-dimensional network structure.<sup>52</sup> In industrial and medical applications, hydrogels have received considerable attention for the development of new controlled delivery systems.<sup>53</sup> Coupling hydrogel and nanoparticles appears to be promising as a new nanoparticulate drug delivery system. Nanoparticle hydrogels have been made with liposomes,<sup>54,55</sup> solid lipid nanoparticles<sup>56,57</sup> and micelles.<sup>58</sup> Nevertheless, all nanoparticle-based hydrogels have been obtained by adding synthetic or natural polymers to induce gelation. These polymers alone led to gel formation and the nanoparticles were dispersed in the matrix, without any interaction with the tridimensional polymer network. The challenge is to limit the addition of polymers to avoid any additional side effects and to simplify the formulation. In this study, rapid gelation was observed once the formulation process was achieved and the gel structure was obtained without the addition of any polymers. The hydrogel property was not found with non-loaded LNCs, but only with the loading of Gem-C12. This drug participated actively in the structuring of the gel.

In the literature, the loading of a lipophilic gemcitabine prodrug into nanoparticles has already been studied, but the gelation effect has never been observed. Zhu used polymeric micelles (at a micelle concentration of 10 mg mL<sup>-1</sup>) for stearyl-modified gemcitabine loading.<sup>59</sup> Cui's group incorporated

stearoyl-modified gemcitabine into nanoemulsions (particle concentrations from 0.5 to 1 mg mL<sup>-1</sup>).<sup>13,16,33</sup> The similar concentrations of Gem-C12-loaded LNCs we developed are in the liquid state and the gel effect was observed at higher concentration levels. The stearyl chain is longer than the lauroyl one and the lipophilicity of the prodrug is certainly improved. Therefore, another explanation of the non-gelation effect could be the location of modified gemcitabine inside the nanoparticle core *versus* the oil–water interface observed in this study. Immordino studied the encapsulation of lipophilic (from valeroyl to stearyl) gemcitabine prodrugs into liposomes.<sup>11</sup> The prodrug, due to the amphiphilic assembly of liposomes, should be located in a similar way to that of LNCs (with the gemcitabine moiety of the prodrug oriented towards the aqueous phase), but the gelation effect was not observed. With liposomes, the prodrug/lipid molar ratio is 0.04 at the maximum. In the present study, gelation was observed at a higher molar prodrug/surfactant ratio (Kol and Span 80), *i.e.* about 0.1, corresponding to a Gem-C12 concentration of 5% (GemC12/Labrafac w/w). The gelation effect is strongly dependent on Gem-C12 and nanocapsule concentrations (Fig. 1 and 2A).

An advantage of a hydrogel drug delivery system is the possibility of directly injecting the preparation. No surgical procedure is required for the insertion of gels into the body and the gels are administered by simple injection.<sup>60</sup> With respect to implantable systems which require light surgery, an injectable hydrogel is particularly attractive. A Gem-C12-loaded LNC hydrogel can be administered in a straightforward manner using a syringe without any loss of viscoelastic gel properties (Fig. 3). Seo used an injectable system containing an anti-cancer drug for the treatment of a primary tumour: B16F10 melanoma cells (*via* intratumoural injection).<sup>61</sup> Cytotoxicity assays have demonstrated the efficiency of GemC12-loaded LNCs on pancreatic and lung cancer cells (Mia PaCa-2, BxPc-3 and H460 cell lines). This was particularly impressive with the Mia Paca-2 cell line which is known to be resistant to gemcitabine.<sup>62</sup> This innovative material could be useful for cancer therapy. To follow the release of LNCs from the gel, *in vitro* dissolutions in PBS at pH 7.4 and pH 6.5 were performed (Fig. 4). The extracellular pH is known to be lower in many tumours than in normal tissue. The extracellular pH of malignant solid tumours is in the range of 6.5 to 6.9, whereas the pH of normal tissues is significantly more alkaline, 7.2 to 7.5.<sup>63,64</sup> No difference of LNC release from hydrogels was observed at both pHs 7.4 and 6.5, with a constant LNC size released throughout the dissolution. However, with 5% of the prodrug (Gem-C12/Labrafac w/w), a slower release was obtained with LNCs of Z-Ave = 55 nm in comparison to 29 nm (100% of hydrogel dissolution at 24 h *vs.* 6 h, respectively). With stronger gel hardness, the hydrogel dissolution was slower (Fig. 4). These experiments showed the possible application of the nanocapsule-based hydrogel as a sustained delivery system after subcutaneous injection and particularly with LNCs (Z-Ave = 55 nm) loaded with 5% of Gem-C12 (Gem-C12/Labrafac w/w). After subcutaneous administration, the Gem-C12-loaded LNC hydrogel should be diluted progressively (Fig. 4) and the Gem-C12-loaded LNCs could passively target the lymph nodes to prevent metastasis as described in Cai's review.<sup>65</sup>

## 4. Conclusion

An innovative nanomedicinal approach was developed for the encapsulation of modified gemcitabine in LNCs. A hydrogel was spontaneously formed depending on the LNC and prodrug concentrations. This material assembly was totally new as far as organogels are concerned, due to the inter-LNC association *via* H-bonds, and this property is directly caused by the prodrug encapsulated at the oil–water interface of the LNC. In addition, after dilution of the material, gemcitabine-loaded LNCs were recovered in suspension in water, with a strong cytotoxic activity with respect to pancreatic and lung cancer cell lines, higher than the native commercialised drug. Current pharmaceutical technology offers the following advantages: (i) it is easy to perform (scale-up possibility); (ii) the gelation reaction occurs rapidly without requiring a template or gelator; (iii) the current study showed that the loaded drug is protected against any degradation process such as deamination; (iv) once diluted, the cytotoxic activity of loaded-LNCs was confirmed, without LNC surface modification; and finally (v) the hydrogel can be injected using a syringe. Using this system for intratumoural or subcutaneous administration could be interesting in the development of new therapeutic practices.

## Acknowledgements

The authors would like to thank Benjamin Siegler (*Plateforme d'Ingénierie et Analyses Moléculaires* (PIAM), Angers, France) for NMR analysis. We also thank the *Service Central d'Analyse* (Solaize, France) for molecular weight and elemental analysis. This work has been carried out within the research programme LYMPHOTARG, supported financially by EuroNanoMed ERANET 09 and by the Région Pays de la Loire.

## References

- 1 E. Moysan, G. Bastiat and J. P. Benoit, *Mol. Pharmacol.*, 2013, **10**(2), 430–444.
- 2 W. Plunkett, P. Huang and V. Gandhi, *Anti-Cancer Drugs*, 1995, **6**(6), 7–13.
- 3 A. M. Bergman, H. M. Pinedo and G. J. Peters, *Drug Resist. Updates*, 2002, **5**(1), 19–33.
- 4 D. R. Rauchwerger, P. S. Firby, D. W. Hedley and M. J. Moore, *Cancer Res.*, 2000, **60**(21), 6075–6079.
- 5 J. J. Farrell, H. Elsaleh, M. Garcia, R. Lai, A. Ammar, W. F. Regine, R. Abrams, A. B. Benson, J. Macdonald, C. E. Cass, A. P. Dicker and J. R. Mackey, *Gastroenterology*, 2009, **136**(1), 187–195.
- 6 J. L. Abbruzzese, R. Grunewald, E. A. Weeks, D. Gravel, T. Adams, B. Nowak, S. Mineishi, P. Tarassoff, W. Satterlee and M. N. Raber, *J. Clin. Oncol.*, 1991, **9**(3), 491–498.
- 7 M. L. Clarke, J. R. Mackey, S. A. Baldwin, J. D. Young and C. E. Cass, *Cancer Treat. Res.*, 2002, **112**, 27–47.
- 8 V. Sebastiani, F. Ricci, B. Rubio-Viqueira, P. Kulesza, C. J. Yeo, M. Hidalgo, A. Klein, D. Laheru and C. A. Iacobuzio-Donahue, *Clin. Cancer Res.*, 2006, **12**(8), 2492–2497.

- 9 B. S. Zhou, P. Tsai, R. Ker, J. Tsai, R. Ho, J. Yu, J. Shih and Y. Yen, *Clin. Exp. Metastasis*, 1998, **16**(1), 43–49.
- 10 L. H. Reddy and P. Couvreur, *Curr. Pharm. Des.*, 2008, **14**(11), 1124–1137.
- 11 M. L. Immordino, P. Brusa, F. Rocco, S. Arpicco, M. Ceruti and L. Cattel, *J. Controlled Release*, 2004, **100**(3), 331–346.
- 12 S. M. Ali, A. R. Khan, M. U. Ahmad, P. Chen, S. Sheikh and I. Ahmad, *Bioorg. Med. Chem. Lett.*, 2005, **15**(10), 2571–2574.
- 13 M. A. Sandoval, B. R. Sloat, D. S. Lansakara-P, A. Kumar, B. L. Rodriguez, K. Kiguchi, J. DiGiovanni and Z. Cui, *J. Controlled Release*, 2012, **157**(2), 287–296.
- 14 C. Celia, D. Cosco, D. Paolino and M. Fresta, *Expert Opin. Drug Delivery*, 2011, **8**(12), 1609–1629.
- 15 B. Pili, L. H. Reddy, C. Bourgaux, S. Lepêtre-Mouelhi, D. Desmaële and P. Couvreur, *Nanoscale*, 2010, **2**(8), 1521–1526.
- 16 W. G. Chung, M. A. Sandoval, B. R. Sloat, D. S. Lansakara-P and Z. Cui, *J. Controlled Release*, 2012, **157**(1), 132–140.
- 17 B. Heurtault, P. Saulnier, B. Pech, J. E. Proust and J. P. Benoit, *Pharm. Res.*, 2002, **19**(6), 875–880.
- 18 B. Heurtault, P. Saulnier, B. Pech, M. C. Venier-Julienne, J. E. Proust, R. Phan-Tan-Luu and J. P. Benoit, *Eur. J. Pharm. Sci.*, 2003, **18**(1), 55–61.
- 19 S. Vrignaud, J. Hureauux, S. Wack, J. P. Benoit and P. Saulnier, *Int. J. Pharm.*, 2012, **436**(1–2), 194–200.
- 20 A. L. Laine, N. T. Huynh, A. Clavreul, J. Balzeau, J. Béjaud, A. Vessieres, J. P. Benoit, J. Eyer and C. Passirani, *Eur. J. Pharm. Biopharm.*, 2012, **81**(3), 690–693.
- 21 E. Allard, F. Hindre, C. Passirani, L. Lemaire, N. Lepareur, N. Noiret, P. Menei and J. P. Benoit, *Eur. J. Nucl. Med. Mol. Imaging*, 2008, **35**(10), 1838–1846.
- 22 C. Vanpouille-Box, F. Lacoëuille, C. Belloche, N. Lepareur, L. Lemaire, J. J. LeJeune, J. P. Benoit, P. Menei, O. F. Couturier, E. Garcion and F. Hindré, *Biomaterials*, 2011, **32**(28), 6781–6790.
- 23 S. David, P. Resnier, A. Guillot, B. Pitard, J. P. Benoit and C. Passirani, *Eur. J. Pharm. Biopharm.*, 2012, **81**(2), 448–452.
- 24 M. Morille, C. Passirani, S. Dufort, G. Bastiat, B. Pitard, J. L. Coll and J. P. Benoit, *Biomaterials*, 2011, **32**(9), 2327–2333.
- 25 A. Paillard, F. Hindré, C. Vignes-Colombeix, J. P. Benoit and E. Garcion, *Biomaterials*, 2010, **31**(29), 7542–7554.
- 26 S. Hirsjärvi, S. Dufort, J. Gravier, I. Texier, Q. Yan, J. Bibette, L. Sancey, V. Josserand, C. Passirani, J. P. Benoit and J. L. Coll, *Nanomed.: Nanotechnol., Biol. Med.*, 2013, **9**(3), 375–387.
- 27 E. Bourseau-Guilmain, J. Béjaud, A. Griveau, N. Lautram, F. Hindré, M. Weyland, J. P. Benoit and E. Garcion, *Int. J. Pharm.*, 2012, **423**(1), 93–101.
- 28 A. Béduneau, P. Saulnier, F. Hindré, A. Clavreul, J. C. Leroux and J. P. Benoit, *Biomaterials*, 2007, **28**(33), 4978–4990.
- 29 B. Heurtault, P. Saulnier, J. E. Proust, B. Pech, J. Richard and J. P. Benoit, *US Pat.*, WO02688000, 2000.
- 30 K. Shinoda and H. Saito, *J. Colloid Interface Sci.*, 1969, **30**(2), 258–263.
- 31 N. Anton, P. Saulnier, C. Gaillard, E. Porcher, S. Vrignaud and J. P. Benoit, *Langmuir*, 2009, **25**(19), 11413–11419.
- 32 S. Vrignaud, J. P. Benoit and P. Saulnier, *Biomaterials*, 2011, **32**(33), 8593–8604.
- 33 B. R. Sloat, M. A. Sandoval, D. Li, W. G. Chung, D. S. Lansakara-P, P. J. Proteau, K. Kiguchi, J. DiGiovanni and Z. Cui, *Int. J. Pharm.*, 2011, **409**(1–2), 278–288.
- 34 X. Shu, K. Zhu and W. Song, *Int. J. Pharm.*, 2001, **212**(1), 19–28.
- 35 S. Hwang, Q. Shao, H. Williams, C. Hilty and Y. Q. Gao, *J. Phys. Chem. B*, 2011, **115**(20), 6653–6660.
- 36 M. Humbert, N. Castéran, S. Letard, K. Hanssens, J. Iovanna, P. Finetti, F. Bertucci, T. Bader, C. D. Mansfield, A. Moussy, O. Hermine and P. Dubreuil, *PLoS One*, 2010, **5**(3), e9430.
- 37 W. Wang, X. Liu, G. Liu, C. Tang, L. Qu and W. Wang, *Chin.-Ger. J. Clin. Oncol.*, 2008, **7**(11), 615–619.
- 38 J. H. Fuhrhop and W. Helfrich, *Chem. Rev.*, 1993, **93**(4), 1565–1582.
- 39 Y. A. Shchipunov, *Russ. Chem. Rev.*, 1997, **66**(4), 301–322.
- 40 S. Murdan, G. Gregoriadis and A. T. Florence, *STP Pharma Sci.*, 1996, **6**(1), 44–48.
- 41 S. Murdan, B. van den Bergh, G. Gregoriadis and A. T. Florence, *J. Pharm. Sci.*, 1999, **88**(6), 615–619.
- 42 S. Murdan, G. Gregoriadis and A. T. Florence, *Int. J. Pharm.*, 1999, **180**(2), 211–214.
- 43 S. Murdan, G. Gregoriadis and A. T. Florence, *J. Pharm. Sci.*, 1999, **88**(6), 608–614.
- 44 S. Pisal, V. Shelke, K. Mahadik and S. Kadam, *AAPS PharmSciTech*, 2004, **5**(4), e63.
- 45 S. Murdan, T. Andryšek and D. Son, *Int. J. Pharm.*, 2005, **300**(1–2), 113–124.
- 46 S. Murdan, G. Gregoriadis and A. T. Florence, *Eur. J. Pharm. Sci.*, 1999, **8**(3), 177–186.
- 47 D. Grace, J. Rogers, K. Skeith and K. Anderson, *J. Rheumatol.*, 1999, **26**(12), 2659–2663.
- 48 P. Mahler, F. Mahler, H. Duruz, M. Ramazzina, V. Liguori and G. Mautone, *Drugs Exp. Clin. Res.*, 2003, **29**(1), 45–52.
- 49 G. Spacca, A. Cacchio, A. Forgács, P. Monteforte and G. Rovetta, *Drugs Exp. Clin. Res.*, 2005, **31**(4), 147–154.
- 50 S. Murdan, G. Gregoriadis and A. T. Florence, *Int. J. Pharm.*, 1999, **183**(1), 47–49.
- 51 C. Bhattacharya, N. Kumar, S. Sagiri, K. Pal and S. Ray, *J. Pharm. BioAllied Sci.*, 2012, **4**(2), 155–163.
- 52 T. R. Hoare and D. S. Kohane, *Polymer*, 2008, **49**(8), 1993–2007.
- 53 D. Seliktar, *Science*, 2012, **336**(6085), 1124–1128.
- 54 N. MacKinnon, G. Guérin, B. Liu, C. C. Gradinaru and P. M. Macdonald, *Langmuir*, 2009, **25**(16), 9413–9423.
- 55 S. Mourtas, S. Fotopoulou, S. Duraj, V. Sfika, C. Tsakiroglou and S. G. Antimisiaris, *Colloids Surf., B*, 2007, **55**(2), 212–221.
- 56 A. C. Silva, M. H. Amaral, E. González-Mira, D. Santos and D. Ferreira, *Colloids Surf., B*, 2012, **93**, 241–248.
- 57 M. A. Casadei, F. Cerreto, S. Cesa, M. Giannuzzo, M. Feeney, C. Marianecchi and P. Paolicelli, *Int. J. Pharm.*, 2006, **325**(1–2), 140–146.
- 58 D. Ma, H. B. Zhang, K. Tu and L. M. Zhang, *Soft Matter*, 2012, **8**(13), 3665–3672.
- 59 S. Zhu, D. S. Lansakara-P, X. Li and Z. Cui, *Bioconjugate Chem.*, 2012, **23**(5), 966–980.

- 60 T. Dipen, P. Amit, P. Vipul P, A. Samir A and D. Tusharbindu R, *American Journal of PharmTech Research*, 2012, **2**(1), 1–13.
- 61 H. W. Seo, D. Y. Kim, D. Y. Kwon, J. S. Kwon, L. M. Jin, B. Lee, J. H. Kim, B. H. Min and M. S. Kim, *Biomaterials*, 2013, **34**(11), 2748–2757.
- 62 D. Chen, M. Niu, X. Jiao, K. Zhang, J. Liang and D. Zhang, *Int. J. Mol. Sci.*, 2012, **13**(1), 1186–1208.
- 63 I. F. Robey, B. K. Baggett, N. D. Kirkpatrick, D. J. Roe, J. Dosesco, B. F. Sloane, A. I. Hashim, D. L. Morse, N. Raghunand, R. A. Gatenby and R. J. Gillies, *Cancer Res.*, 2009, **69**(6), 2260–2268.
- 64 E. K. Rofstad, B. Mathiesen, K. Kindem and K. Galappathi, *Cancer Res.*, 2006, **66**(13), 6699–6707.
- 65 S. Cai, Q. Yang, T. R. Bagby and M. L. Forrest, *Adv. Drug Delivery Rev.*, 2011, **63**(10–11), 901–908.